J Therm Anal Calorim (2015) 119:499–506
DOI 10.1007/s10973-014-4122-7

Thermal stability of magnetic nanoparticles coated by blends of modified chitosan and poly(quaternary ammonium) salt

Marta Ziegler-Borowska · Dorota Chełminiak · Halina Kaczmarek

Received: 13 May 2014 / Accepted: 21 August 2014 / Published online: 9 September 2014

Abstract Magnetite nanoparticles (Fe_3O_4 NPs) coated by modified chitosan (m-CS) rich of amino groups and its mixture with poly[*N*-benzyl-2-(methacryloxy)-*N*,*N*-dimethylethanaminium bromide] (PQ) with various mass ratios were prepared by co-precipitation method. The thermal stability of magnetic materials has been investigated by thermogravimetric analysis (TG/DTG/DTA) in air and nitrogen atmosphere. It was found that magnetic NPs coated by polymer blend were characterized by lower thermal stability than protected only by alone CS or m-CS. Magnetite NPs enhance thermooxidative degradation of polymers, however, the stable surface layer, formed from polymer degradation products, efficiently protects the magnetite transformation at higher temperatures. The content of magnetite in obtained systems has been also determined from TG curves.

Keywords Magnetite nanoparticles · Modified chitosan · [*N*-Benzyl-2-(methacryloxy)-*N*,*N*-dimethylethanaminium bromide] · Thermogravimetric analysis

Introduction

Hybrid materials based on magnetite nanoparticles (Fe_3O_4, NPs) coated by polymers have attracted a great interest due to their superparamagnetic properties and various biomedical applications (e.g., in magnetic resonance imaging contrast enhancement, tissue repair, immunoassay, detoxification of biological fluids, hyperthermia, drugs delivery, and cells separation) [1].

One of the most common coatings of magnetic NPs is chitosan (CS), linear polysaccharide characterized by several important advantages: biodegradability, biocompatibility, and biocide properties. Owing to the presence of reactive functional groups (OH and NH_2) in each CS unit, it can be applied for binding of therapeutics, targeting ligands, and imaging agents [2, 3].

Over the last decade, many reports have been focused on preparation CS-coated magnetic NPs [4, 5]. The recent work concerns the CS modification leading to increase of amine group amount in polysaccharide chains [6]. It facilitates the intermolecular interactions with bioactive molecules and broadens the potential applications of magnetic materials in modern biotechnology. Besides the CS modification by direct chemical reaction, the physical blending with other components is also practices. One possibility is using of amphiphilic polymer as the second coating component. An example can be poly(cationic) salt containing quaternary ammonium groups in side substituents. Such permanently, positively charged polyelectrolytes are characterized by good solubility in water and high ability to bind of bioactive compounds. They are also known as antimicrobials and disinfectants.

Recently, the simple and effective method of synthesis of magnetite NPs coated by mixture of CS and amphiphilic polyionic methacrylate (PQ) has been elaborated [7, 8]. The obtained magnetic NPs were useful in process of enzyme immobilization, thus, it seems to be a very promising material for application in advanced biotechnology and medicine.

The aim of this work was to study the thermal stability of magnetite NPs coated by the mixture of modified CS (m-CS) and cationic polymer (PQ) in comparison to magnetic NPs covered by CS or m-CS alone.

Applying oxygen-free, neutral atmosphere (N_2) for thermogravimetry (TG), the thermal decomposition of magnetite coating will be studied, while, in air atmosphere, the behavior of materials in used conditions at elevated temperatures can be determined.

M. Ziegler-Borowska · D. Chełminiak · H. Kaczmarek (✉)
Faculty of Chemistry, Nicolaus Copernicus University, Gagarina 7 Street, 87-100 Toruń, Poland
e-mail: halina@chem.uni.torun.pl; halina@chem.umk.pl

Experimental

Materials and synthesis

All reagents for synthesis [iron(II) chloride tetrahydrate, iron(III) chloride hexahydrate, CS (low molecular mass, deacetylation degree = 75–85 %), glutaraldehyde, acetic acid, sodium hydroxide, sodium periodate, benzyl bromide, 2-(dimethylamino)ethylmethacrylate, ethylenediamine, epichlorohydrin], and solvents have been supplied by Sigma Aldrich and used without any purification.

The CS modification has been done by hydroxyl groups reaction with epichlorohydrin, sodium periodate, glutaraldehyde, and finally with ethylenediamine leading to CS rich of long-distanced amino groups.

Amphiphilic polymer containing quaternary ammonium groups: poly[*N*-benzyl-2-(methacryloxy)-*N*,*N*-dimethylethanaminium bromide] (PQ) has been obtained by early reported procedure [7, 8].

The chemical structure of obtained polymers was confirmed by FTIR and ^{1}H-NMR spectroscopy. The details of synthesis method and structure characterization of obtained materials are included in other submitted article [6].

Coated magnetite NPs were obtained by in situ method from solution of iron salts: $FeCl_2$, $FeCl_3$ containing polymer during gradual precipitation by NaOH. The m-CS–PQ blends with two various components mass ratios (1:1 and 1:5) have been used. The mean size of obtained magnetic particles, determined by SEM and TEM, was approximately 20–25 nm. Moreover, the presence of Fe_3O_4 has been confirmed by XRD analysis [6].

TG analysis

The thermal properties of the CS, m-CS, PQ, and synthesized magnetite NPs coated by polymers were studied using SDT 2960 Simultaneous DSC–TGA thermogravimetric system. The ~5 mg samples were heated from room temperature to 800 °C at a heating rate of 10 °C min^{-1}, in air and nitrogen atmosphere, at gas flow rate of 100 mL min^{-1}.

The following parameters were determined for each step from TG curves: T_o: temperature of the degradation onset (°C), T_{max}: temperature at the maximum process rate (°C), Δm: mass loss (%), carbonaceous residue (%) at 800 °C, and temperature at 20 % mass loss of polymer was calculated ($T_{20\ \%}$).

Results and discussion

The magnetite NPs were covered by different polymeric systems: virgin CS, m-CS, as well as two blends of polycationic methacrylate (PQ) and m-CS with 1:1 and 1:5 mass ratios. The CS was chemically modified for the purpose of introduction of additional amine groups in polysaccharide chains allowing for better adhesion to proteins or enzymes in the case of predicted biomedical applications. Introduction of the second amphiphilic polymer (PQ) to NPs coating leads to improvement of solubility in water and better stability of colloidal solutions. The structures of polymers used for magnetite coating are shown in Fig. 1.

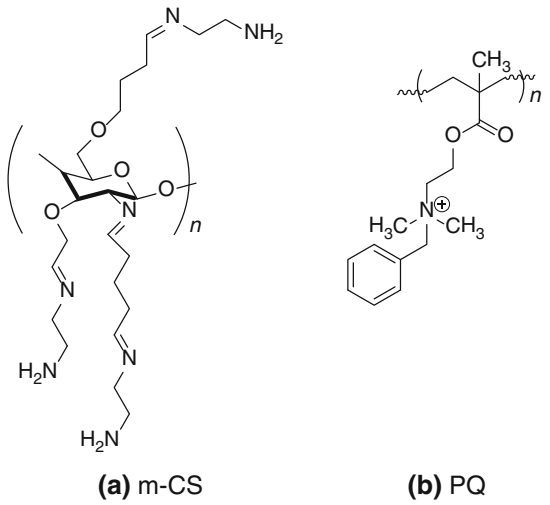

Fig. 1 Chemical structure of modified chitosan (m-CS) and poly[*N*-benzyl-2-(methacryloxy)-*N*,*N*-dimethylethanaminium bromide] (PQ)

The composition and spectral characterization of coated NPs has been the subject of previous work [6] but still no information on the thermal behavior of these systems. The results of TG analysis for all applied polymers (points Sections 'Chitosan (CS)', 'Modified chitosan (m-CS)', 'Poly[*N*-benzyl-2-(methacryloxy)-*N*,*N*-dimethylethanaminium bromide] (PQ)') and coated NPs (Sections 'Thermal stability of magnetite NPs coated by modified chitosan (m-CS) and its blends with polycationic methacrylate (m-CS–PQ) in nitrogen atmosphere', 'Thermal stability of magnetite NPs coated by modified chitosan (m-CS) and its blends with polycationic methacrylate (m-CS–PQ) in air atmosphere') are discussed below. Because the thermal degradation of studied systems is very complicated, all curves can be divided into three main ranges (I: 20–130/200 °C, II: 130/200–330/400 °C and III: 330/400–800 °C), even if any stage is composed of two or more less clear, overlapped processes.

Chitosan (CS)

TG curve of CS in nitrogen atmosphere shows two degradation stages at 20–160 and 160–400 °C ranges

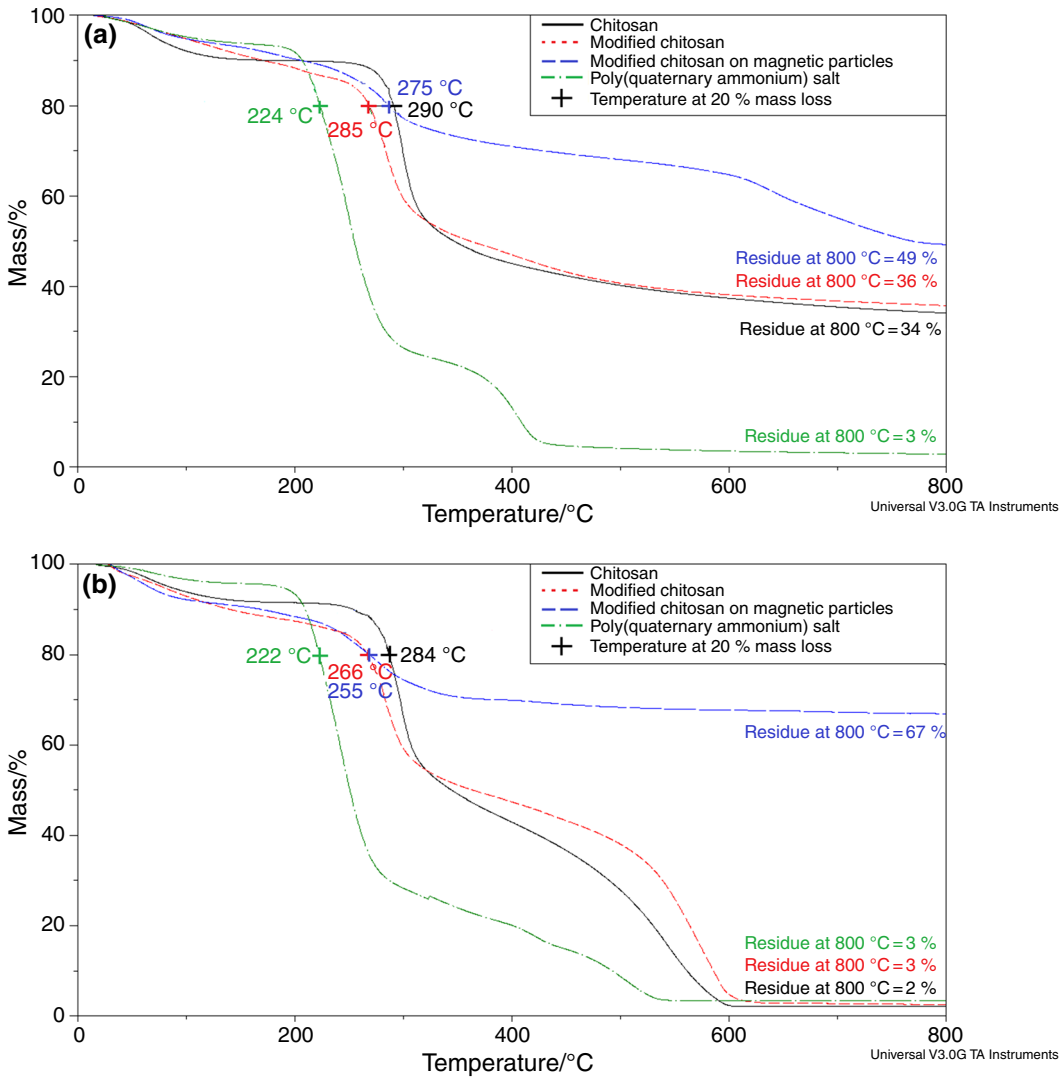

Fig. 2 TG curves of chitosan, modified chitosan, poly(quaternary ammonium) salt, and chitosan on magnetic particles in **a** nitrogen atmosphere and **b** air atmosphere

(Figs. 2a, 3a). In the first one, about 10 % mass loss is observed, which is attributed to the evolution of water adsorbed by polymer. The maximum rate of this process occurs at 64 °C. The second stage is a main decomposition of CS which starts about 210 °C (maximum rate at 298 °C). The 44 % mass loss in this stage is connected to the rupture of polysaccharide chains (including dehydration, deamination, deacetylation, breaking of glycoside bonds, and pyranose ring opening), vaporization, and elimination of degradation products [9–11]. Above 400 °C, further slow decrease of mass loss (without any maximum at DTG) is observed up to 800 °C.

It was found that first stage is an endothermic process (with minimum at DTA at 64 °C), which can be explained by the breaking of hydrogen bonds followed by water evaporation. Such effect was observed in all studied samples.

The second main process is connected with small exothermic effect (maximum at 306 °C), reported also by other researchers [12]. Such behavior of CS during thermal degradation in nitrogen indicates its relatively high deacetylation degree [13].

In air atmosphere, the CS decomposes in three degradation stages (Figs. 2b, 3b): the first one—at 20–160 °C range with a mass loss of 9 % and T_{max} at 63 °C; the second—at 220–400 °C with Δm of 48 % (T_{max} = 298 °C) and third—at 395–600 °C with Δm of 41 % (T_{max} = 541 °C). According to knowledge on CS thermo-oxidative degradation [14], these steps can be attributed to water evaporation, main decomposition (oxidation and decay of oxidized CS),

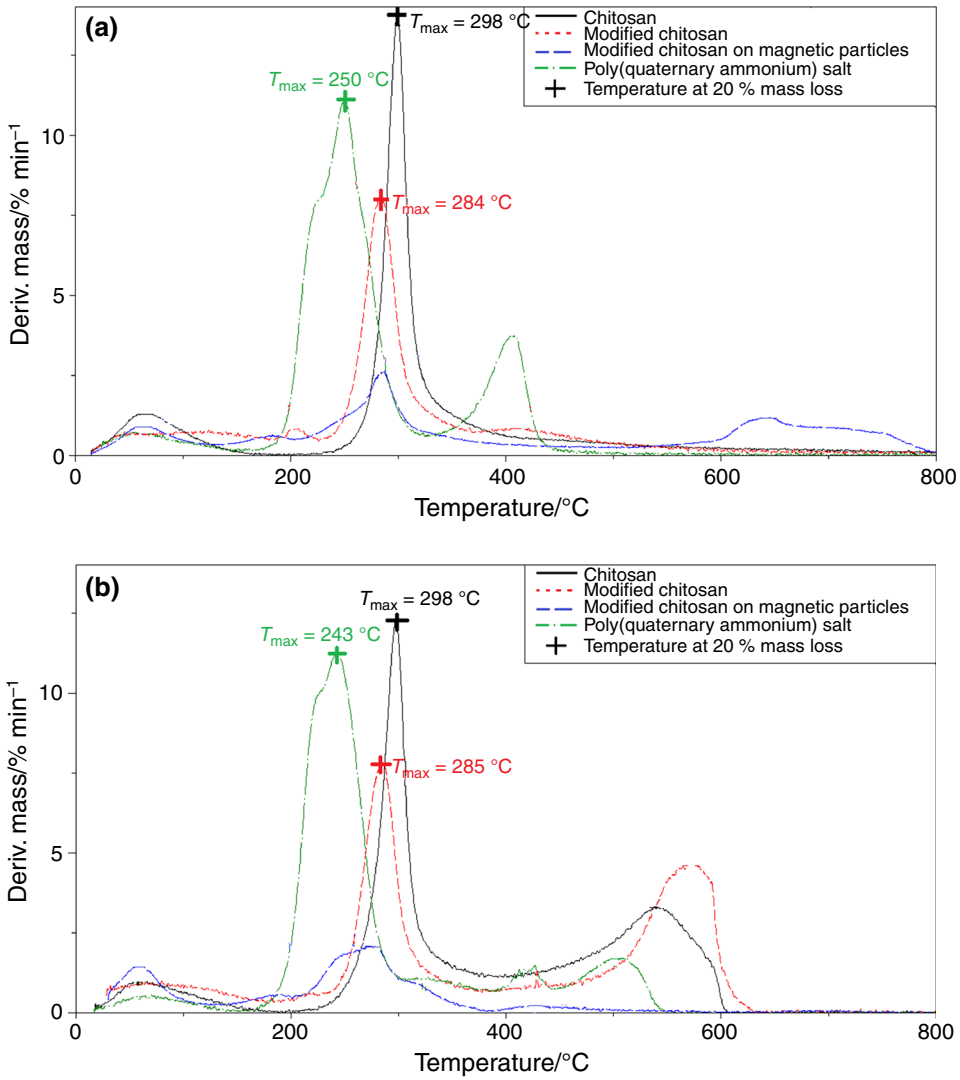

Fig. 3 DTG curves of chitosan, modified chitosan, poly(quaternary ammonium) salt, and chitosan on magnetic particles in **a** nitrogen atmosphere and **b** air atmosphere

and final, almost total volatilization of decomposed at early stages macromolecules.

DTA of CS recorded in air shows two exothermic peaks at about 300 and 540 °C (more intensive and broader than the first one) which confirm oxidation accompanying thermal degradation (in the second and third stage) and small endothermic effect at the beginning of decomposition (∼50 °C) due to the moisture removing.

The polymer residue at 800 °C is 34 and 2 % in nitrogen and air, respectively. Relatively high amount of remained carbonizate in N_2 suggests that thermally stable degradation products appear resulting of free radical recombination. Besides of cross-linked chains, also polyaromatic structures can be found in carbonaceous residue [15]. During the degradation in air, formation of intermediates rich in oxygen is expected at early stages. Particularly, unstable are peroxides and hydroperoxides, which finally decompose completely at higher temperatures. CS TG analysis is in good accordance to previous literature data [16–18].

Modified CS (m-CS)

TG curves of m-CS are somewhat different than those for unmodified CS (Figs. 2, 3). TG for m-CS recorded in nitrogen shows low but systematic mass loss up to 190 °C ($\Delta m \approx 12$ %) followed by the fast decomposition process at ≈200–370 °C range ($\Delta m \approx 40$ %). This second process is not uniform—two small peaks (at 204 and 421 °C) appear closely to main maximum at 284 °C. Then, at higher temperatures (450–800 °C) again slow evolution of gaseous products is observed ($\Delta m \approx 12$ %). It suggests that volatile products containing nitrogen are formed during whole process at studied temperature range. The lack of clear step at low temperature (<100 °C), typical for water evaporation from hydrophilic polymers, indicates that CS after modification becomes less susceptible to moisture adsorption. It is connected with the significant decrease of hydroxyl groups' amount in CS resulting of substitution of side chains with NH_2 ends. In fact, it was proved that water

molecules stronger interact with CS hydroxyl groups than with the amine groups [19, 20]. Lower ability to water adhesion is also caused by the presence of longer aliphatic side chains (containing four–seven C atoms).

The main step of m-CS decomposition starts at lower temperature; moreover T_{max} is also lower comparing to these parameters for unmodified CS. It was expected because C–N bonds are weaker comparing to C–C and C–O [21].

The exothermic peak at main decomposition step is similar to found for CS but slightly shifted to lower temperature (295 °C) and less sharp.

Thermal degradation of m-CS in air occurs also in three clear stages, similarly to CS decomposed in oxidative conditions. Taking into account the main degradation process (at 200–400 °C range), it can be concluded that m-CS heated in air is also less stable than unmodified polysaccharide. However, the last stage (at 400–600 °C range), connected with decomposition of oxidized products, occurs later ($T_{max} \approx 570$ °C) than in CS ($T_{max} \approx 541$ °C). The decomposition of m-CS in air is almost completed at 800 °C. The second and third stage is connected with exothermic oxidation.

The differences in TG curves of CS and m-CS confirm the chemical modification of polymer, which was previously stated by other methods [6].

Poly[*N*-benzyl-2-(methacryloxy)-*N*,*N*-dimethylethanaminium bromide] (PQ)

The thermal degradation of this amphiphilic polymer occurs in three stages. The shape of TG curves is also dependent on experiment atmosphere (Figs. 2, 3).

The first, small decomposition step (at temperature lower than 150 °C) attributed to water evaporation is less efficient in air than that in nitrogen.

The second, main stage of polymer decomposition at temperature range of 160–330 °C (with about 70 % mass loss) is similar in both atmospheres. Only small shift of T_{max} toward lower temperature is observed for PQ degraded in air.

The third, degradation stage in N_2 (temperature range 330–450 °C, $T_{max} = 407$ °C, $\Delta m = 21$ %) is significantly faster than in air. Moreover, in air atmosphere the additional peak with maximum rate at 507 °C appeared. The broad exotherms were found in both experiments but the shape of DTA curve is different in N_2 and in air. It can be caused the presence of unsaturated bonds in CS side chains undergoing addition reaction. In inert atmosphere, it can be a direct cross-linking between two C=N groups and formation of cyclic structures, while in air, the addition of oxygen and formation of peroxide bridges is possible. Then, such structures also decompose completely due to instability of O–O groups.

Almost total (95 %) decomposition of PQ in N_2 is observed already at 450 °C, while in air only about 550 °C.

Thermal stability of magnetite NPs coated by m-CS and its blends with polycationic methacrylate (m-CS–PQ) in nitrogen atmosphere

TG curves of magnetite NPs coated with polymeric blends are presented in Fig. 4. In nitrogen atmosphere, two stages with maximum rate at 62 and 181 °C are observed below 200 °C. Taking into account that CS does not decompose at such low temperatures, both monitored DTG peaks and corresponding mass loss (7 %) are attributed to excretion of non-bonded and bonded water. Because peak at 181 °C is absent in DTG of alone m-CS, it looks that the magnetite NPs are responsible for the strong bonding of water. It should be added that water acts as plasticizer in CS but in its blends it additionally plays a role of compatibilizer [22].

The next steps at 200–500 and 500–800 °C ranges with corresponding mass loss of 28 and 16 %, respectively, can be attributed to polymer main chain scission and decomposition of more stable degradation products (formed at earlier stages).

In magnetite NPs coated by m-CS–PQ blend, temperature at maximum process rate (T_{max}) is shifted to lower temperatures, while the onset temperature (T_o) is the same for the second (main) degradation stage. The mass loss in I and III step is somewhat higher comparing to this parameter in CS, m-CS, and PQ alone, while in the II stage the trend is opposite.

The third stage (450–800 °C) is also complex: two clear maxima at DTG appeared but their intensity (i.e., process rates) is dependent on the CS content. In the case of m-CS and m-CS–PQ (1:1) coating, the peak component at about 640 °C is dominant, whereas in NPs covered by 1:5 m-CS–PQ blend, the peak at about 700 °C is stronger. This last decomposition stage (>500 °C) is noteworthy because it does not occur in pure polymers. It clearly indicates that this effect is connected with the presence of magnetite NPs and can be explained by decomposition of macromolecules (strictly speaking—theirs degradation products) strongly bonded to NPs surface.

DTA curves reveal that the energy is systematically released during thermal degradation of magnetite NPs coated by polymeric blends. Small deflection on DTA curve corresponding to maximum rate of the last decomposing process is observed in all three types of samples.

The carbonaceous residue at 800 °C is almost the same in all studied polymer-magnetite specimens (49–51 %).

Taking into account that residue of free m-CS and PQ in this temperature is 36 and 3 %, respectively, the content of magnetite in nanocomposites can be estimated. Hence, in NPs with 1:1 blend coating is about 30 mass% Fe_3O_4 and

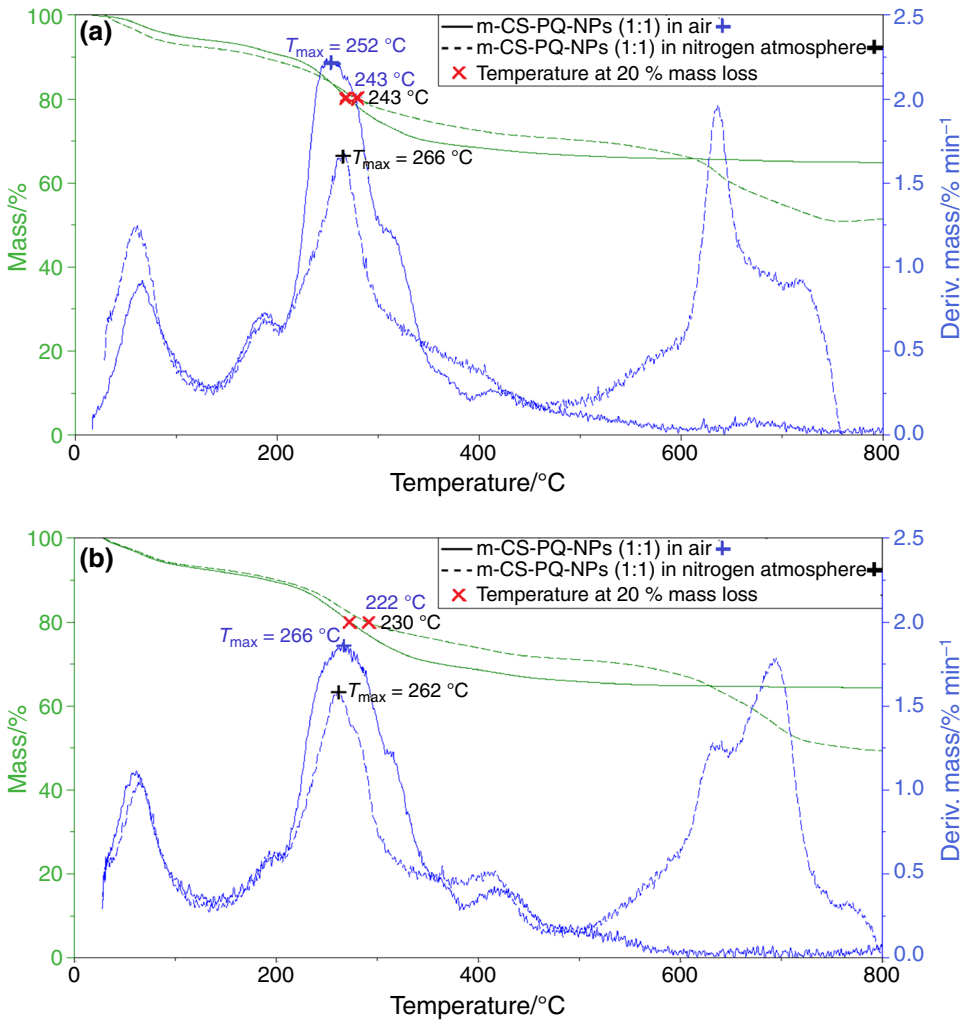

Fig. 4 TG/DTG of magnetite nanoparticles coated by blend of modified chitosan and poly(quaternary ammonium) salt **a** m-CS–PQ–NPs 1:1 and **b** m-CS–PQ–NPs 1:5, in air and nitrogen atmosphere

about 40 mass% in magnetite covered by 1:5 blend. In the sample with m-CS coating, the magnetite content, estimated by direct subtraction of coal residues at 800 °C, is only 13 %. It suggests that protecting blend layer is much thinner than m-CS coating.

Thermal stability of magnetite NPs coated by m-CS and its blends with polycationic methacrylate (m-CS–PQ) in air atmosphere

In oxidative atmosphere, two main decomposition steps (and third: minor) are recorded (Fig. 4). The first step is connected not only with water evaporation but also with decomposition of side chains containing C=N bonds in m-CS.

The second stage, starting at 130 °C, is due to oxidative degradation of polymeric coating. Besides of classical oxidation of macromolecules, the addition of oxygen to unsaturated bonds is very probable. Strong exothermic peaks on DTA curves confirm this assumption.

The small shifting of TG curves and T_{max} indicates that the NPs coated by polymer blend are less stable than NPs covered by m-CS only.

The carbonaceous residue at 800 °C in air for all magnetic samples (64–67 %) is much higher than those parameters' obtained in N_2. It means that very stable, oxidized, and crosslinked products are formed at NPs surface.

Interestingly, at higher temperatures (>500 °C), no effects on TG, DTG, and DTA curves were observed. It means that thermally stable carbonaceous coating was formed at the NPs surface, which additionally protects the magnetite against further transformation and oxidation, at least till 800 °C.

Final remarks: the effect of magnetite NPs, sample composition, and atmosphere on polymer thermal degradation

On the base of characteristic temperatures determined from TG curves, it can be concluded that magnetite NPs

Table 1 The temperature at 20 % mass loss of polymer ($T_{20\ \%}$) for studied systems during heating at nitrogen and air atmosphere

Samples	$T_{20\ \%}$/°C	
	Nitrogen atmosphere	Air atmosphere
CS	290	284
m-CS	285	266
PQ	224	222
NPs + m-CS	275	255
NPs + m-CS–PQ (1:1)	243	243
NPs + m-CS–PQ (1:5)	230	222

decrease thermal stability of CS but this effect depends on atmosphere during heating. Similar effects caused by inert (argon) and air atmosphere on thermal degradation of dextran-coated magnetite have been recently reported [23].

In nitrogen, characteristic temperatures (T_o and T_{max}) in the NPs covered by blends are almost the same. However, simple unequivocal conclusion is difficult because the first stage and the second stage partly overlap. Thus, it is impossible to determine precisely T_o and temperature of the end of considered degradation stages.

Because there is no simple correlation of thermal stability with the composition of polymer coating, the additional parameter: the temperature corresponding to 20 % mass loss of polymer was calculated ($T_{20\ \%}$) for clarification of results (Table 1). For the magnetite NPs, these values were calculated after subtraction of magnetite mass from the total sample mass.

As can be seen, the modification of CS leads to the decrease of its thermal stability. The second polymer used for coating modification is much less thermally stable than both CS and m-CS.

Obtained $T_{20\ \%}$ values clearly indicate that magnetite NPs coated by m-CS alone are characterized by somewhat better thermal stability than NPs coated by blends (1:1 and 1:5). The higher content of amphiphilic polymer (PQ) in the coating blend makes the lower resistance to heat.

Thermal stability of coated NPs in air is lower than that in nitrogen atmosphere with the exception of m-CS + PQ (1:1) blend, where $T_{20\ \%}$ is exactly the same.

Conclusions

The m-CS and polyamphiphilic polymer blend were applied for obtaining of magnetite coating ensuring demanded physico-chemical properties. The TG analysis of these novel magnetic systems revealed that their thermal properties depend on the coating composition and atmosphere.

The content of Fe_3O_4 in NPs + m-CS, NPs + m-CS–PQ (1:1), and NPs + m-CS–PQ (1:5), determined from TG, was about 13, 30, and 40 %, respectively.

The thermal degradation of polymer-coated NPs in nitrogen atmosphere takes places in three stages process, while in air occurs in two main steps. Magnetite NPs coated by m-CS–PQ blends are characterized by lower thermal stability than coated by CS alone. However, observed thermal properties do not disqualify these materials in biomedical applications.

Other interesting result of this work is formation of thermally resistant surface layer on magnetite NPs in air atmosphere. It is composed of oxidized, crosslinked carbonaceous polymeric residue, which protects further phase transition of Fe_3O_4 to maghemite or hematite (no exothermic effect above 450 °C). The ability of polymer to crosslinking increases with PQ content in the blend because this polymer contains unsaturated C=N groups in side chains.

The behavior of such novel functional systems during heating is important for broadening their application as superparamagnetic hybrid materials in various modern technology branches (for example, in catalysis). The knowledge on the thermal stability of biopolymer-based materials also allows determining the possible processing techniques.

References

1. Gupta AK, Gupta M. Synthesis and surface engineering of iron oxide nanoparticles for biomedical applications. Biomaterials. 2005;26:3995–4021.
2. Hong S, Chang Y, Rhee I. Chitosan-coated ferrite (Fe_3O_4) nanoparticles as a T2 contrast agent for magnetic resonance imaging. J Korean Phys Soc. 2010;56:868–73.
3. Mucha M. Chitozan wszechstronny polimer ze źródeł odnawialnych. Warszawa: WNT; 2010.
4. Elmizadeh H, Khanmohammadi M, Ghasemi K, Hassanzadeh G, Nassiri-Asl M, Garmarudi AB. Preparation and optimization of chitosan nanoparticles and magnetic chitosan nanoparticles as delivery systems using Box–Behnken statistical design. J Pharm Biomed Anal. 2013;80:141–6.
5. Unsoy G, Yalcin S, Khodadust R, Gunduz G, Gunduz U. Synthesis optimization and characterization of chitosan coated iron oxide nanoparticles produced for biomedical applications. J Nanopart Res. 2012;14:964–73.
6. Ziegler-Borowska M, Chełminiak D, Siódmiak T, Sikora A, Marszałł MP, Kaczmarek H. Synthesis of chitosan coated magnetic nanoparticles with surface modified with long-distanced amino groups as a bioligands carrier. Mater Lett. 2014;132:53–65.
7. Siódmiak T, Ziegler-Borowska M, Marszałł MP. Lipase-immobilized magnetic chitosan nanoparticles for kinetic resolution of (*R*,*S*)-ibuprofen. J Mol Catal B. 2013;94:7–14.
8. Ziegler-Borowska M, Siódmiak T, Chełminiak D, Cyganiuk A, Marszałł MP. Magnetic nanoparticles with surfaces modified with chitosan-poly[*N*-benzyl-2-(methacryloxy)-*N*,*N*-dimethylethanaminium bromide] for lipase immobilization. Appl Surf Sci. 2014;288:641–8.

9. De Britto D, Compana-Filho SP. Kinetics of the thermal degradation of chitosan. Thermochim Acta. 2007;465:73–82.
10. Pereira MAV, Fonseca GD, Silva-Junior AA, Fernandes-Pedrosa MF, De Moura MFV, Barbosa EG, Gomes APB, Dos Santos KSCR. Compatibility study between chitosan and pharmaceutical excipients used in solid dosage forms. J Therm Anal Calorim. 2014;116:1091–100.
11. Pereira FS, Da Silva Agostini DL, Job AE, Gonzalez ERP. Thermal studies of chitin–chitosan derivatives. J Therm Anal Calorim. 2013;114:321–7.
12. Li W, Xiao L, Qin C. The characterization and thermal investigation of chitosan–Fe_3O_4 nanoparticles synthesized via a novel one-step modifying process. J Macromol Sci Pure Appl Chem. 2011;48:57–64.
13. Nam YS, Park WH, Ihm D, Hudson SM. Effect of the degree of deacetylation on the thermal decomposition of chitin and chitosan nanofibers. Carbohydr Polym. 2010;80:291–5.
14. Ou ChY, Li SD, Yang L, Li ChP, Hong PZ, She XD. The impact of cupric ion on thermo-oxidative degradation of chitosan. Polym Int. 2010;59:1110–5.
15. Zawadzki J, Kaczmarek H. Thermal treatment of chitosan in various conditions. Carbohydr Polym. 2010;80:394–400.
16. Lopez FA, Merce LR, Alguacil FJ, Lopez-Delgado A. A kinetic study on the thermal behavior of chitosan. J Therm Anal Calorim. 2008;91:633–9.
17. Diab MA, El-Sonbati AZ, Bader DMD. Thermal stability and degradation of chitosan modified by benzophenone. Spectrochim Acta A. 2011;79:1057–62.
18. Hong PZ, Li SD, Ou ChY, Li ChP, Yang L, Zhang ChH. Thermogravimetric analysis of chitosan. J Appl Polym Sci. 2007;105:547–51.
19. Rudea DR, Secall TK, Bayer RK. Differences in the interaction of water with starch and chitosan films as revealed by infrared spectroscopy and differential scanning calorimetry. Carbohydr Polym. 1999;40:49–56.
20. Neto CGT, Giacometti JA, Job AE, Ferreira FC, Fonseca JLC, Pereira MR. Thermal analysis of chitosan based networks. Carbohydr Polym. 2005;62:97–103.
21. Weast RC. CRC handbook of chemistry and physics. 69th ed. Boca Raton: CRC; 1989.
22. Mucha M, Pawlak A. Thermal analysis of chitosan and its blends. Thermochim Acta. 2005;427:69–76.
23. Carp O, Patron L, Culita DC, Budrugeac P, Feder M, Diamandescu L. Thermal analysis of two types dextran-coated magnetite. J Therm Anal Calorim. 2010;101:181–7.